Available online at www.sciencedirect.com
ScienceDirect
Carbohydrate Polymers 65 (2006) 469–478
Carbohydrate Polymers
www.elsevier.com/locate/carbpol

Yield stress components of waxy corn starch–xanthan mixtures: Effect of xanthan concentration and different starches

Piyada Achayuthakan [a], Manop Suphantharika [a], M.A. Rao [b,*]

[a] Department of Biotechnology, Faculty of Science, Mahidol University, Rama 6 Road, Bangkok 10400, Thailand
[b] Department of Food Science and Technology, Cornell University, Geneva, NY 14456-0462, USA

Received 17 November 2005; received in revised form 1 February 2006; accepted 6 February 2006
Available online 3 April 2006

Abstract

Yield stress of 6% (w/w) waxy maize (WXM), cross-linked waxy maize (CLWM), and cold water swelling (CWS) starches in xanthan gum dispersions: 0%, 0.35%, 0.50%, 0.70%, and 1.0% was measured with the vane method at an apparent shear rate of 0.05 s^{-1}. The intrinsic viscosity of the xanthan gum was determined to be: 112.3 dL/g in distilled water at 25 °C. Values of the static (σ_{0s}) and dynamic (σ_{0d}) yield stress of each dispersion were measured before and after breaking down its structure under continuous shear, respectively. The WXM and CWS starches exhibited synergistic behavior, whereas the CLWM starch showed antagonistic effect with xanthan gum. The difference ($\sigma_{0s} - \sigma_{0d}$) was the stress required to break the inter-particle bonding (σ_b). The contributions of the viscous (σ_v) and network (σ_n) components were estimated from an energy balance model. In general, values of σ_b of the starch–xanthan gum dispersions decreased and those of σ_n increased with increase in xanthan gum concentration.

Keywords: Starch; Xanthan gum; Vane yield stress; Components of yield stress

1. Introduction

Experimental studies on mono disperse rigid particles, molecular dynamic simulations, and statistical mechanical theories, as well as structural or phenomenological approaches have contributed to the better understanding of the rheological behavior of concentrated disperse systems. Efforts in the latter category include those of Casson (1959); van den Tempel (1961) and Michaels and Bolger (1962). Their application to complex systems requires few restrictive assumptions and much useful information can be obtained. For example, the model of Casson (1959) developed for printing inks, has been found to be applicable to several complex food systems. Likewise, the structural model of Michaels and Bolger (1962) for dispersions of particle flocs that associate to form weakly bonded aggregates and tenuous networks, giving rise to plastic properties, was found to be useful to understand fermentation broths (Metz, Kossen, & Suijdam, 1979).

Yield stress is the minimum stress required to initiate flow and is one measure of the strength of a network of interacting particles. Extrapolation of shear flow data to zero shear rate is a popular indirect means of estimation of yield stress; shear stress (σ) versus shear rate ($\dot{\gamma}$) data is fitted to a constitutive equation, such as the Herschel-Bulkley Eq. (1) or the Casson Eq. (2) models:

$$\sigma = \sigma_{0H} + K_H \dot{\gamma}^{n_H}, \tag{1}$$

$$\sqrt{\sigma} = \sqrt{\sigma_{0C}} + \sqrt{\eta_\infty \dot{\gamma}}, \tag{2}$$

where K_H is the consistency index, n_H is the flow behavior index, η_∞ is the infinite shear rate viscosity, and σ_{0H} and σ_{0C} are the Herschel-Bulkley and Casson yield stresses, respectively. The value of yield stress so obtained is largely influenced by the quality and quantity of data at low shear rates, and the model selected to fit the data and the range of shear rates where it is applied.

* Corresponding author. Tel.: +1 315 521 9252; fax: +1 315 787 2284.
E-mail address: mar2@cornell.edu (M.A. Rao).

0144-8617/$ - see front matter © 2006 Elsevier Ltd. All rights reserved.
doi:10.1016/j.carbpol.2006.02.007

Nomenclature

c	concentration (%)
D	diameter of the paddle (mm)
H	height of the paddle (mm)
k	constant in Eq. (9)
K_H	consistency coefficient (Pa s^n)
k_s	proportionality constant between rotational speed and shear rate (/rev)
K	vane parameter (m^3)
n_H	flow behavior index (dimensionless)
N	rotational speed (rpm)
t	time (s)
T	torque exerted on the vane (N m)
T_m	maximum value of torque (N m)

Greek Letters

$\dot{\gamma}$	shear rate (1/s)
η_α	viscosity at infinite shear rate (Pa s)
η	apparent viscosity (Pa s)
η_{sp}	specific viscosity (Pa s)
θ	angular deformation (rad)
σ	shear stress (Pa)
σ_0	total yield stress, from vane data, (Pa)
σ_{0C}	Casson yield stress (Pa)
σ_{0d}	dynamic yield stress (Pa)
σ_{0H}	Herschel-Bulkley yield stress (Pa)
σ_{0s}	static yield stress (Pa)
σ_b	stress required to break the internal bonds, from vane data, (Pa)
σ_n	stress required to break the aggregate network, from vane data, (Pa)
σ_v	stress due to purely viscous drag, from vane data, (Pa)

Because of minimum disruption of structure and no wall-slip, the vane test is a reliable and a direct method of measurement of yield stress. A vane with at least four blades is fully immersed in the sample and rotated slowly at a constant speed until the torque reaches a maximum value (T_m) and the sample yields (Dzuy & Boger, 1983) and then relaxes to an equilibrium value. The yield stress (σ_0) is calculated using Eqs. (3) and (4):

$$\sigma_0 = K^{-1} T_m, \tag{3}$$

where K is the vane parameter that depends on the diameter (D) and height (H) of the vane:

$$K = \frac{\pi D^3}{2}\left(\frac{H}{D} + \frac{1}{3}\right). \tag{4}$$

Based on the work of Michaels and Bolger (1962), from an energy balance at the point of maximum deformation (yield point) in the vane test, the contributions of different structural components to the total yield stress can be estimated (Genovese & Rao, 2003a):

$$\sigma_0 = \sigma_b + \sigma_v + \sigma_n, \tag{5}$$

$$\sigma_0 = \sigma_{0s}, \tag{6}$$

$$\sigma_b = \sigma_{0s} - \sigma_{0d}, \tag{7}$$

$$\sigma_v = \eta_\infty \dot{\gamma}, \tag{8}$$

where, σ_b is the stress required to break the bonds between the flocs, σ_v is the stress dissipated due to purely viscous drag, and σ_n is the stress required to break the aggregate network; σ_{0s} and σ_{0d} are the static and dynamic yield stresses of the samples with undisrupted and disrupted structure, respectively. Additional discussion of the yield stress components can be found in Genovese and Rao (2005).

Starch is a major source of energy for humans. It is composed of amylose and amylopectin that coexist in the form of granules; amylose is a linear chain of α (1 → 4) D-glucopyranosyl units with a few branches and amylopectin has a main backbone of α (1 → 4) D-glucopyranosyl units and α (1 → 6) D-glucopyranosyl branch points. In contrast to native cornstarch that contains ~25% amylose, waxy cornstarch has less than 2% amylose. It is called 'waxy' because it appears waxy or shiny when the grains are cut (Whistler & BeMiller, 1997). Cross-linking of waxy starch adds chemical bonds at random locations within granules which stabilize and strengthen the relatively tender swollen starch granules (Langan, 1986). Cold water swelling (CWS) starch can be created by treating a native starch with alcohol at high temperatures and pressures (Eastman & Moore, 1984) or with an alcohol–alkali mixture (Chen & Jane, 1994), followed by drying. CWS granules are larger than native starch granules, remain intact, and the starch can be used in dessert formulations, controlled drug-release, and to thicken foods for consumption by dysphagia patients (Meng & Rao, 2005).

The mechanical properties of starch dispersions and gels are affected by the physical properties of the dispersed phase and continuous phase, and the volume fraction of granules (Bagley & Christianson, 1982; Genovese & Rao, 2003b; Miles, Morris, Orford, & Ring, 1985; Ring & Stainsby, 1982) that in turn are affected by protocols used. Therefore, considerable care is required in preparing starch dispersions (Genovese & Rao, 2003a; Okechukwu & Rao, 1995). Because the granules are compressible, their volume fractions in heated starch dispersions are difficult to measure accurately (Rao, 1999). Therefore, the mass fraction of the starch granules, cQ, is determined, where c is the concentration (w/w) of dry starch, and Q is the mass of swollen starch granules per unit mass of dry starch. Determination of values of cQ of starch-in-xanthan gum dispersions would be much more difficult than of starch-in-water

dispersions due to the complex interactions between starch and xanthan gum.

Xanthan gum is an extracellular microbial polysaccharide produced from *Xanthomonas campestris* found on leaves of plants of the cabbage family and has found many applications in the food industry (Whistler & BeMiller, 1997). It has a cellulose backbone with trisaccharide sidechains of two mannoses and one glucuronic acid for alternate glucose unit of a main chain and a high molecular weight due to its rigid rod structure. It is well known that the viscosity of a polymer solution, such as that of xanthan gum, is dependent on the concentration of the polymer and its molecular weight (MW). Instead of MW, one can use the intrinsic viscosity $[\eta]$ as a useful indicator of the MW of a gum (Rao, 1999).

Many studies have been conducted on the structural aspects and rheology of starch–xanthan gum dispersions. Here, studies related to the present work are discussed. With addition of xanthan gum, dramatic changes in mobility were observed prior to gelatinization of corn, waxy corn, and potato starches indicating adsorption of the gum on the starch granule surface; this result was confirmed by confocal scanning laser microscopy (Gonera & Cornillon, 2002). Krüger, Ferrero, and Zaritzky (2003) reported that the mean starch granule diameter in 10% w/w native cornstarch after heating at 84.5 °C for 20 min was 31.7 μm. The diameters in 10% native cornstarch with 15% w/w sucrose, and with 15% w/w sucrose and 1% w/w xanthan gum were 25.7 and 23.9 μm, respectively. They suggested that starch granule swelling was reduced by the presence of gums because of lower heating rates and the reduced mobility of water molecules.

The yield stress and apparent Young's modulus of mixtures of potato starch (10–15%) and xanthan gum (0.1% and 0.3%) were mainly influenced by ageing time of the gel and starch concentration; the temperature of preparation and xanthan concentration had less pronounced effects on overall rheology (Mandala & Palogou, 2003).

From amylograms of 5.64% wheat starch in water and in 0.5% xanthan gum, Christianson, Hodge, Osborne, and Detroy (1981) concluded that the viscosity of the latter significantly increased at 80–94 °C. Paste consistency was attributed to interactions of solubilized starch, gum, and swollen starch granules. The viscoelastic properties of the pastes and gels of 4% corn starch pasted in the presence of 0.1–0.5% of guar gum, locust bean gum or xanthan gum properties were primarily governed by the volume fraction of the swollen granules (Alloncle & Doublier, 1991). The additional contribution of the continuous phase was due to its viscoelastic properties and the effects experienced with xanthan gum were stronger than with guar and locust bean gums. Increasing the xanthan concentration in waxy corn starch–xanthan gum blends increased their intrinsic viscosity in 90% (v/v) dimethylsulphoxide and 10% (v/v) water and decreased the coil overlap concentration markedly (Wang, Sun, & Wang, 2001).

Few studies have been conducted on the vane yield stress of dispersions of different starches in xanthan gum. Because such dispersions are complex systems, we have undertaken a phenomenological analysis of their yield stress values. The objective of this study was to examine the role of structural components on yield stress of dispersions of waxy maize starch (WXM), cross-linked waxy maize starch (CLWM), and cold water swelling (CWS) starch in xanthan gum; the components indicate contributions to yield stress due to bonding, network, and viscous forces. None of the starches contained more than a trace of amylose so that the starch–xanthan gum interactions were not influenced by amylose. While it is necessary to heat the dispersions of WXM and CLWM starches for their granules to gelatinize and swell, those of CWS starch expand without heating.

2. Materials and methods

2.1. Materials

Waxy maize starch (Amioca, batch HC8190), cross-linked waxy maize starch (Purity® W, batch# BD5429), and cold water swelling maize starch (Ultra-Tex® HV, batch# KC7117) were donated by the National Starch and Chemical Co. (Bridgewater, NJ, USA). Xanthan gum (Batch 1 D0535A) was purchased from CP Kelco Company (San Diego, CA, USA).

2.2. Moisture content

The moisture content of the starch and gum powders was determined by heating weighed samples at 105 °C overnight, cooled in a desiccator 30 min, and weighed for the dry weight.

2.3. Intrinsic viscosity of xanthan gum

A Cannon-Ubbelohde Dilution Capillary Viscometer of size 50 (Cannon Instrument Co., State College, PA, USA), was used to determine the intrinsic viscosity of xanthan gum dispersions at 25 °C. The efflux times of distilled water and of xanthan gum dispersions ranging in concentrations from 0.005% to 0.02% were measured in triplicate and averaged. When values of specific viscosity divided by xanthan concentration (η_{sp}/c) were plotted against xanthan gum concentration (c, %), they followed Huggins' equation (figure not shown):

$$\frac{\eta_{sp}}{c} = [\eta] + k_1[\eta]^2 c, \tag{9}$$

where k_1 is the interaction coefficient.

2.4. Preparation of heated starch–xanthan gum dispersions

Dispersions of xanthan gum, whose intrinsic viscosity was determined earlier, were prepared with concentrations

of 0.35%, 0.5%, 0.70%, and 1.0%. A weighed amount of xanthan gum was sprinkled into the vortex of 300 g of distilled water and stirred by a magnetic stirrer for 30 min. Then, the dispersion was mixed manually with a glass rod to eliminate 'fish-eyes' of the gum that are sticky particles containing undissolved gum inside and wet gum outside. The xanthan gum dispersion was kept in a refrigerator overnight to allow air bubbles to escape and to fully disperse the xanthan gum.

Based on the protocols developed for studies on starch-in-water dispersions (Genovese & Rao, 2003a; Okechukwu & Rao, 1995), a procedure was developed to instantaneously heat 6% WMS and CLWM starch dispersions at a fixed temperature. Essentially, the procedure involved adding xanthan gum dispersion at a high temperature (92 °C) to a small amount of starch-in-water dispersion at a lower temperature so that the resulting mixture attained instantaneously 80 °C, the desired heating temperature. The xanthan-starch dispersion was heated at 80 °C for 10 min in a rotating round-bottom flask immersed in a water bath (Rotavapor, Buchi, Switzerland); after heating, the dispersion was cooled in a water–ice bath until the temperature decreased to less than 30 °C. For CWS dispersions, weighed amounts of xanthan gum and CWS starch dispersions were carefully mixed under gentle stirring at ambient temperature and kept in the refrigerator overnight for complete hydration.

2.5. Vane rheometer

A six-blade star-shaped vane (diameter = 40 mm and height = 60 mm) (Qiu & Rao, 1988) attached to a Rotovisco RV30 viscometer (Haake, Newington, NH, USA) was used to determine, in order: the static yield stress (σ_{0s}), the flow curve over 0–90 s^{-1}, and the dynamic yield stress (σ_{0d}). Values of σ_{0s} and σ_{0d} at the apparent shear rate 0.05 s^{-1}, and shear rate-shear stress of the flow curve were determined as described earlier (Genovese & Rao, 2003a). The dispersion to be tested was poured slowly into a jacketed stainless steel vessel (inner diameter = 72 mm and height = 110 mm). The temperature in the vessel was controlled at 20.0 ± 0.1 °C by circulating water from a constant temperature bath (Haake, Newington, NH, USA).

The vane was slowly inserted completely into the test sample and left for 1 h for the sample's temperature and structure stabilizing. First, the static yield stress was measured at the apparent shear rate, 0.05 s^{-1}. The changing values of the measured torque (T) as a function of time were recorded using the computer software Rotation RV30, version 3, of Haake (Newington, NH, USA). The vane yield stress (σ_0) was calculated from the measured maximum torque (T_m) using Eqs. (3) and (4). The angular deformation (θ) of the sample at the point of failure was calculated as

$$\theta = \frac{2\pi}{60} N.t, \tag{10}$$

where N is the vane rotational speed (rpm) and t is the time (s) required to reach the maximum torque. Next, to obtain apparent shear rate versus shear stress data, the vane was programmed to ramp the shear rate from 0 to 90 s^{-1} (up curve) followed immediately by the down curve from 90 to 0 s^{-1}. Vane-apparent shear rate values were calculated assuming that the average apparent shear rate ($\dot{\gamma}$) around the paddle was directly proportional to N (Rao & Cooley, 1984):

$$\dot{\gamma} = k_s \frac{N}{60}, \tag{11}$$

where k_s is a constant that must be determined for each vane (Rao, 1999). The value of k_s for the paddle used in this work was determined earlier (Qiu & Rao, 1988) to be 11.6/rev. Recognizing that the shear stress is directly proportional to the torque, $\sigma = A * T$, the proportionality constant A was calculated by measuring T vs. $\dot{\gamma}$ for four different Brookfield Viscosity Standards (Brookfield Engineering Laboratories, Inc., Stoughton, MA, USA) with magnitudes ranging from 0.492 to 11.78 Pa s (Genovese & Rao, 2003a).

After the sample was sheared, its dynamic yield stress was also determined as described earlier. The Casson model Eq. (2) was fit to the flow data and values of the model's parameters were determined using linear regression on the square roots of apparent shear rate and shear stress. The contribution of the network component (σ_n) was calculated using Eq. (5), after the bonding (σ_b) and viscous (σ_v) components of the yield stress were calculated using Eqs. (7) and (8), respectively.

2.6. Granule size distributions

Granule size distributions of the starch and the starch–xanthan mixtures were determined using a laser diffraction particle size analyzer (Coulter® LS130, Coulter Corporation, Miami, FL). The heated mixtures containing starch were diluted 10-fold with distilled water; the dispersions were gently stirred manually with a glass rod in order to disperse the starch granules. The mixtures were added to the sample vessel until the polarization intensity differential scattering (PIDS) was more than 45. The refractive indices were set at 1.33 for distilled water and 1.529 for the dispersed phase. The absorption of dispersed phase was set at 0.1 (Nayouf, Loisel, & Doublier, 2003).

3. Results and discussion

3.1. Intrinsic viscosity of xanthan

From the viscosity measurements on dilute xanthan dispersions in water, using the Huggins equation [see Eq. (9)], the intrinsic viscosity of xanthan was calculate to be 112.3 dL/g in distilled water at 25 °C. Given that a high value of intrinsic viscosity of xanthan in water can be expected (Launay, Cuvelier, & Martinez-Reyes, 1984), this

value is considered to be reasonable. Values of the coil overlap parameter, $c[\eta]$, for the xanthan concentrations: 0.35%, 0.50%, 0.70%, and 1.0% are: 3.93, 5.62, 7.86, and 11.23, respectively.

3.2. Starch granule size distribution

Figs. 1–3 reveal subtle differences in the size distributions of the starch granules in the dispersions of WXM, CLWM, and CWS starches in xanthan, respectively. Large differences can be seen in the size distributions of WXM granules at low and high apparent diameter values (Fig. 1). In contrast, all the CWS starch dispersions (Fig. 2) exhibited nearly identical granule size distribution. The CLWM starch dispersions (Fig. 3) exhibited granule size distributions that were affected at the high apparent diameter values, especially at xanthan concentrations 0.35% and 0.5%. From the granule size distribution data, because of increase in starch granule size of WXM–xanthan and CLWM–xanthan mixtures, it appears that availability of water for starch gelatinization and swelling was not limited.

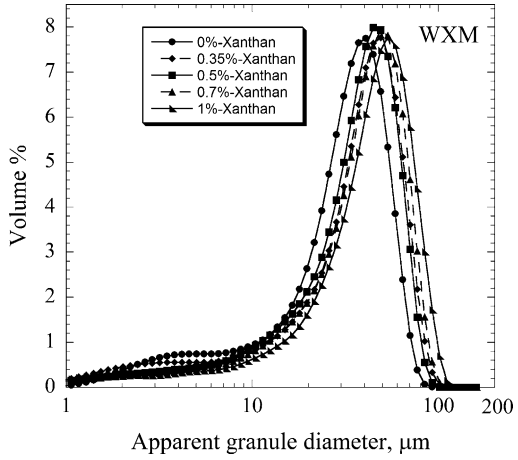

Fig. 1. Large differences can be seen in the size distributions of waxy maize starch (WXM) granules at low and high apparent diameter values.

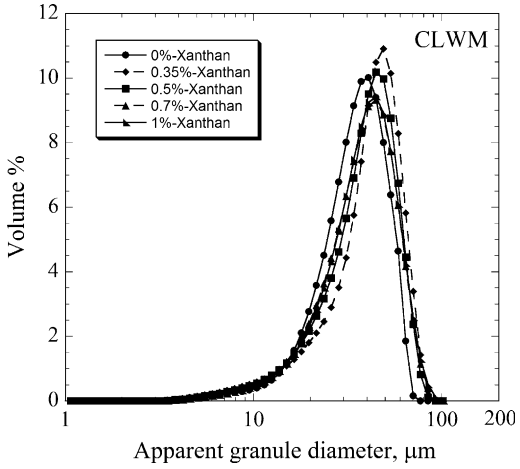

Fig. 2. The cold water swelling (CWS) starch dispersions exhibited nearly identical granule size distributions.

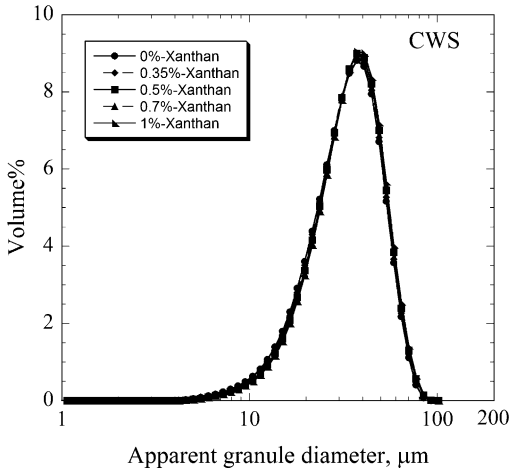

Fig. 3. The cross-linked waxy maize (CLWM) starch dispersions exhibited granule size distributions that were affected at the high xanthan concentrations: 0.7% and 1.0%.

3.3. Stress versus time results

For the purpose of illustration, the vane stress versus time curves of waxy maize starch (WXM) dispersion in water (0% x) and at the xanthan concentrations 0.35%, 0.5%, 0.7%, and 1% with undisrupted (u) and disrupted (d) structure are shown in Fig. 4. Similar stress versus time curves were shown by the xanthan, the CLWM starch–xanthan, and the CWS starch–xanthan dispersions, and they are not shown here. Values of the static and dynamic yield stresses, as well as those of the components: bonding, network, and viscous are tabulated in Table 1.

3.4. Yield stress of waxy maize starch–xanthan dispersions

Xanthan gum and WXM starch lack gelling properties. However, they can form entanglement networks by weak

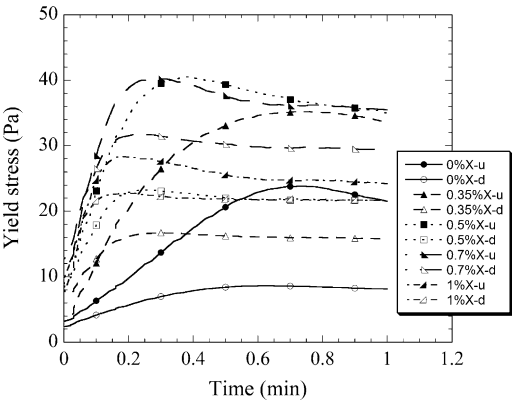

Fig. 4. The stress versus time curves for static yield stress and dynamic yield stress of waxy maize (WXM) starch–xanthan gum dispersions are shown.

Table 1
Static and dynamic yield stresses, and the components: bonding, viscous, and network xanthan gum and starch–xanthan mixtures

Starch	Xanthan concentration (%)	Static YS (Pa)	Dynamic YS (Pa)	Bonding YS (Pa)	Viscous YS (Pa)	Network YS (Pa)
Starch, 0%	0.35	1.9	1.4	0.50	0.006	1.4
	0.50	3.5	2.0	1.5	0.007	2.0
	0.70	5.1	2.3	2.8	0.010	2.3
	1.00	8.6	3.1	5.5	0.014	3.1
WXM, 6%	0.00	23.9	8.6	15.3	0.037	8.6
	0.35	36.6	16.7	19.9	0.033	16.7
	0.50	40.5	23.3	17.2	0.034	23.2
	0.70	40.2	31.8	8.4	0.030	31.8
	1.00	28.4	22.7	5.7	0.014	22.7
CLWM, 6%	0.00	59.3	45.3	14.0	0.101	45.0
	0.35	59.0	56.3	2.6	0.013	56.3
	0.50	33.4	33.0	0.38	0.013	33.0
	0.70	35.2	38.1	−2.9	0.012	38.1
	1.00	31.7	28.2	3.5	0.010	28.2
CWS, 6%	0.00	39.2	27.1	12.1	0.041	27.0
	0.35	56.4	45.9	10.5	0.018	45.9
	0.50	58.1	44.1	14.0	0.016	44.1
	0.70	55.6	42.1	13.5	0.015	42.0
	1.00	58.6	41.1	17.5	0.017	41.0

Starch concentration was fixed at 6%. The abbreviations WXM, CLWM, and CWS indicate waxy maize starch, cross-linked waxy maize starch, and cold-water swelling starch, respectively.

bonds between the xanthan gum chains or between the outer short chains of amylopectin (Nguyen, Jensen, & Kristensen, 1998). Eidam, Kulicke, Kuhn, and Stute (1995) concluded that the formation of junction zones from cross-links of native cornstarch network was inhibited by the presence of xanthan gum. The presence of xanthan in continuous phase may have interrupted amylose network due to incompatibility of the two polymers resulting in phase separation. However, the mechanism applicable to waxy maize starch and xanthan network is still not clear. The yield stresses of waxy maize starch and waxy maize starch–xanthan gum mixture, especially their bonding and network components, may explain the network formed.

The static yield stress of WXM starch dispersion in water was 23.9 Pa. Values of the static yield stresses of WXM starch–xanthan dispersions at xanthan concentrations 0.35%, 0.5%, 0.7%, and 1% were 36.6, 40.5, 40.2, and 28.4 Pa, respectively (Fig. 1). Static yield stress of the dispersion with 0.35% xanthan increased 53% compared with that of the starch–water dispersion and it increased by 11% when xanthan concentration was increased from 0.35% to 0.5%. However, it decreased slightly when xanthan concentration was increased to 0.7% and significantly at 1% xanthan concentration.

Values of the bonding component of yield stress (σ_b) of the WXM starch–xanthan dispersions at 0.35% and 0.5% xanthan concentration were higher than that of the starch–water dispersion by 30% and 13%, respectively. Thus, addition of xanthan at the indicated levels promoted inter-particle bonding in the dispersions. However, at the higher xanthan concentrations: 0.7% and 1.0%, the opposite trend was observed, i.e., values of the σ_b decreased while those of the network component (σ_n) increased. When the xanthan concentration was increased to 1%, there was a decrease in values of both the static and dynamic yield stresses, and $\sigma_n > \sigma_b$.

3.5. Yield stress of cross-linked waxy maize starch–xanthan dispersions

Compared to static and dynamic yield stresses of CLWM starch–water dispersion, those of CLWM–xanthan mixtures were lower (Table 1). Unlike with the aforementioned WXM–xanthan and the CWS–xanthan dispersions, to be discussed next, the static and dynamic yield stresses of CLWM–xanthan dispersions decreased with addition of xanthan. This result appears to be due to a decrease in the effectiveness of xanthan to augment the network structure of the CLWM starch granules in the dispersions. Interestingly, the inter-particle bonding, σ_b, decreased with addition of xanthan; this result is surprising because the inter-particle bonding of pure xanthan dispersions increased with concentration of the gum. Most of the yield stress of a CLWM starch–xanthan mixture was due to its network. At xanthan concentrations 0.35–1.0, values of σ_n of the CLWM starch–xanthan mixtures were nearly constant at about 33 ± 5 Pa. Given that the magnitude of σ_n depends on the number and nature of the particles (Metz et al., 1979), it appears that the nature of the CLWM starch granules did not change much.

Tattiyakul and Rao (2000) reported that CLWM–water dispersions exhibited antithixotropic flow behavior in the shear stress range less than about 120–150 Pa. From Fig. 5, it can be seen that CLWM–xanthan dispersions also exhibited such behavior, especially at the xanthan

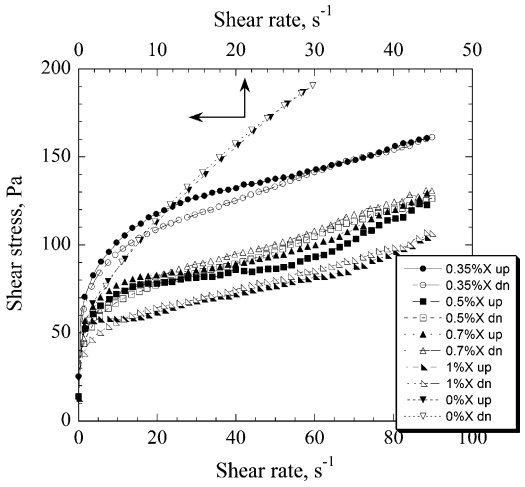

Fig. 5. Shear rate versus shear stress data on cross-linked waxy maize (CLWM) starch–xanthan gum mixtures shows that antithixotropic behavior of the dispersions: values of shear stress of the down curves were higher than those of the up curves.

concentrations 0.50%, 0.70%, and 1.0%. Thus, these data also indicate that the presence of xanthan gum did not alter the nature of the starch granules and, hence, the flow behavior of the CLWM–xanthan dispersions.

3.6. Yield stress of cold water swelling starch–xanthan dispersions

As the name indicates, granules of the CWS corn starch swell without heating. Compared to the yield stress of the CWS corn starch–water dispersions, addition of 0.35% xanthan resulted in a large increase in both the static and dynamic yield stresses. However, using higher concentrations of xanthan: 0.5%, 0.70%, and to 1.0%CWS did not result in corresponding increases in yield stress (Table 1).

3.7. Assessment of interaction of starch–xanthan dispersions

Given that both the xanthan dispersions at the specific concentrations used and the 6% dispersions of the starches in water exhibited yield stresses, it was possible to determine if there were synergistic or antagonistic interactions. Table 2 contains the static yield stresses of the xanthan dispersions in water (Column A), of the three starches in water (Column B) and their sum (Column C), and those of the mixed starch–xanthan dispersions (Column D). One can say that there is synergism between xanthan and starch if values in Column D are higher than those in Column C; if they are lower, there is antagonism. From Table 2, it seems that WXM (except with 1% xanthan concentration) and CWS starches exhibited synergistic interaction with xanthan, while CLWM starch–xanthan dispersions exhibited antagonistic behavior. The lack of synergism between CLWM starch and xanthan is also evident in the lower values of shear stress and, by inference, apparent viscosity (Fig. 5).

In Fig. 6, the values of yield stress of the starch–xanthan dispersions relative to those of the starch–water dispersions (YS/YS0) and relative mean granule diameters (D/D0) are plotted against values of $c[\eta]$ of xanthan gum. Again, with values of YS/YS0 less than 1.0, the lack of synergism between CLWM starch and xanthan gum is evident. In addition, it appears that the mean starch granule diameters obtained from the size distributions do not reflect accurately the subtle differences in the distributions (Figs. 1–3).

The effect of xanthan gum on the relative contribution of components of yield stress of the mixed dispersions is

Table 2
Comparison of static yield stresses, Pa, (YSS) of starch–water and starch–xanthan gum mixtures

Starch	Xanthan concentration (%)	YSS xanthan (A)	YSS starch–water (B)	$C = A + B$	YSS starch–xanthan (D)	$D - C$	Interaction
WXM	0.00	—	23.9	23.9	23.9	0.0	—
	0.35	1.9	23.9	25.7	36.6	10.9	S
	0.50	3.5	23.9	27.4	40.5	13.1	S
	0.70	5.1	23.9	28.9	40.2	11.3	S
	1.00	8.6	23.9	32.5	28.4	−4.1	A
CLWM	0.00	—	59.3	59.3	59.3	0.0	—
	0.35	1.9	59.3	61.2	59.0	−2.2	A
	0.50	3.5	59.3	62.9	33.4	−29.5	A
	0.70	5.1	59.3	64.4	35.2	−29.2	A
	1.00	8.6	59.3	68.0	31.7	−36.3	A
CWS	0.00	—	39.2	39.2	39.2	0.0	—
	0.35	1.9	39.2	41.1	56.4	15.3	S
	0.50	3.5	39.2	42.7	58.1	15.4	S
	0.70	5.1	39.2	44.3	55.6	11.3	S
	1.00	8.6	39.2	47.8	58.6	10.7	S

A = static yield stress of xanthan gum dispersion.
B = static yield stress of each starch dispersion.
$C = A + B$.
D = static yield stress of starch–xanthan dispersion.
Interaction = S (synergistic), A (antagonistic), − no interaction.

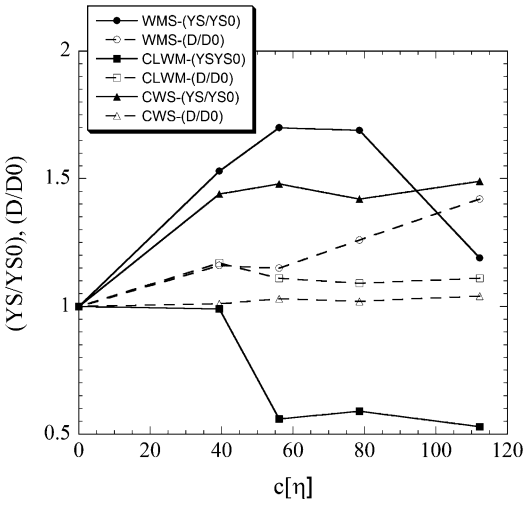

Fig. 6. Values of yield stress of the starch–xanthan dispersions relative to those of the starch–water dispersions (YS/YS0) and relative mean granule diameters (D/D0) plotted against values of $c[\eta]$ of xanthan gum.

also of interest. In Fig. 7, it can be seen that in general addition of xanthan lowered the percent contribution of inter-particle bonding and a concomitant increase in the mixed system network's contribution. However, the results were different for each starch dispersion: inter-particle bonding in WXM dispersions was higher than in CWS and CLWM starches at low xanthan concentrations, that in CWS starch was nearly constant at all xanthan concentrations, and that in CLWM starch dispersions was lower than in the other two starches. The relatively low inter-particle bonding in CLWM starch dispersions in water is in agreement with results of Genovese and Rao (2003a). For the xanthan–water dispersions, the percent contribution of inter-particle bonding increased with increase in its concentration, which in turn may have contributed to the slight increase in inter-particle bonding of CLWM and CWS starch dispersions at the higher xanthan concentration (Fig. 7).

Increase in association of starch granules in the presence of xanthan (Abdulmola, Hember, Richardson, & Morris, 1996) appears to have contributed to the synergism in the CWS–xanthan and WXM–xanthan dispersions (Table 2). Further, the decrease in the relative contribution of inter-particle bonding due to addition of xanthan (Fig. 7) suggests that those associations were weak and decreased with xanthan concentration.

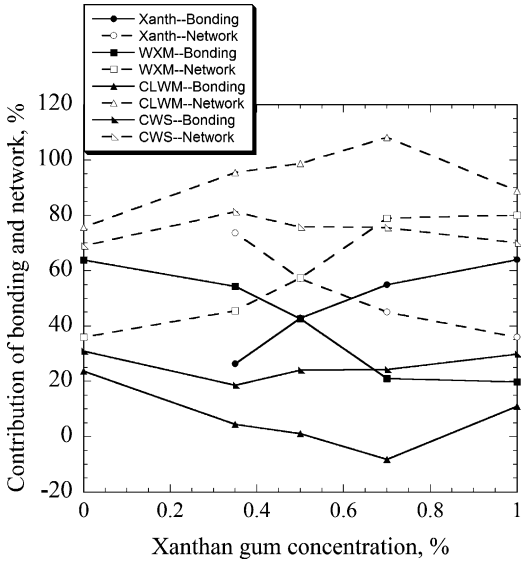

Fig. 7. Contributions of bonding and network to yield stress of xanthan gum and its mixtures with waxy maize starch (WXM), cross-linked waxy maize starch (CLWM), and cold-water swelling (CWS) starches. Also shown are data on the water dispersions of those starches.

3.8. Texture map

Mandala, Palogou, and Kostaropoulos (2002) reported that addition of xanthan gum increased the hardness of 12% soluble potato starch gels; the hardness increased when xanthan concentration was increased from 0.1% to 0.3%. The static and dynamic yield stresses of the various dispersions are plotted against the corresponding values of deformation at which failure occurred to obtain a texture map (Fig. 8). The pure xanthan gum and the WXM dispersions fall between rubbery and tough, while those containing CLWM and CWS starches are between brittle and tough. The former also exhibited relatively large angular deformations at failure whose values decreased with increase in xanthan concentration: the xanthan dispersions from 0.4 to 1.2 red, and the WXM–xanthan dispersions from 0.3 to 1.2 red. The undisrupted dispersions containing CLWM and CWS starches are close to being brittle, while the disrupted dispersions shifted towards tough category. Both the undisrupted and disrupted dispersions containing CLWM and CWS starches had relatively small angular deformations at failure, 0.1 to 0.2 red, whose values did not change in a systematic manner with xanthan concentration.

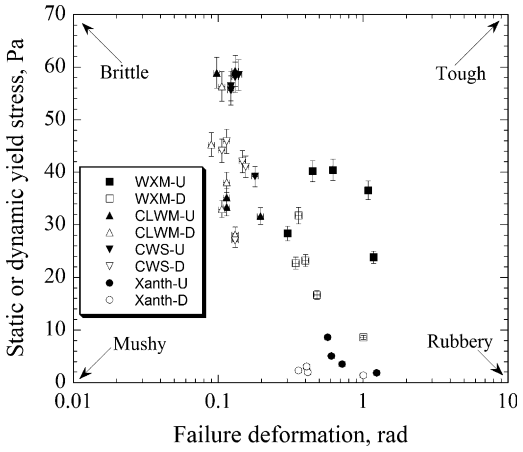

Fig. 8. Static and dynamic yield stresses of the studied dispersions plotted against the corresponding values of deformation at failure.

3.9. Results based on flow behavior and viscosity

It was of interest to study trends shown by rheological parameters other than vane yield stress. Values of the Hershel-Bulkley model Eq. (1) were determined by non-linear regression of the down flow curves of the studied dispersions, similar to those of CLWM starch (Fig. 5). Because of the scatter in data and their different ranges of shear rates, as well as that they were obtained by curve fitting, these values allow qualitative evaluation of the dispersions. For example, all the starch dispersions and starch–xanthan mixtures exhibited shear thinning behavior ($n_H < 1$) and values of yield stress, σ_{0H}, were much lower (0.002–5.4 Pa) than those obtained by the vane method. The consistency coefficient, K_H, of dispersions of WXM starch increased with concentration of xanthan from 1.2 Pa s^n (0% xanthan) to 2.5 Pa s^n (1.0% xanthan), of CLWM starch decreased from 6.9 Pa s^n (0% xanthan) to 2.0 Pa s^n (1.0% xanthan), and of CWS starch remained constant at about 2.2 Pa s^n.

Christianson et al. (1981) attributed increase in wheat starch–xanthan amylograph viscosity during gelatinization to interactions of amylose, gum, and swollen starch granules, and the subsequent stable viscosity was attributed to amylose–gum interaction. In the absence of amylose in the studied systems, entanglement networks by weak bonds among the xanthan gum chains or between the outer short chains of amylopectin may again explain increase in values of K_H of WXM starch dispersions. The decrease in values of K_H of dispersions of CLWM starch and the constant values of CWS starch are in agreement with trends in yield stress.

Values of viscous component of yield stress, that are based on infinite shear viscosity, η_∞, estimated using the Casson model Eq. (2) were too low to decipher differences among them with confidence (Table 1); those of WXM starch and its mixtures with xanthan showed no significant difference, while those of CLWM and CWS starches were lower than pure starch (Table 1).

4. Conclusion

Unlike heated dispersions of WXM and CLWM starches, granule size distributions of CWS starch and CWS starch–xanthan gum mixtures were not different. Thus, one may assume that the effect of xanthan addition on starch granule size distribution of WXM and CLWM starches occurred during pasting by heating. Xanthan gum had synergistic effect on yield stress of WXM and CWS starch dispersions. In the CWS-0.35% xanthan gum mixtures, values of yield stress did not change with xanthan concentration. However, it had antagonistic effect on yield stress of CLWM starch dispersions. Increasing xanthan concentration resulted in increase in the yield stress of WXM starch dispersions.

Acknowledgements

Financial support from the Thailand Research Fund through the Royal Golden Jubilee Ph.D. Program (Grant No. PHD/0117/2546) to P.A. and M.S. is acknowledged. This research work was also partially supported by the Higher Education Development Project and the USDA Regional Research Project NC 136. We thank National Starch and Chemical Co. for providing all starches used in this study.

References

Abdulmola, N. A., Hember, M. W. N., Richardson, R. K., & Morris, E. R. (1996). Effect of xanthan on the small-deformation rheology of cross-linked and uncross linked waxy maize starch. *Carbohydrate Polymers, 31*(1/2), 65–78.

Alloncle, M., & Doublier, J. L. (1991). Viscoelastic properties of maize starch/hydrocolloid pastes and gels. *Food Hydrocolloids, 5*, 455–467.

Bagley, E. B., & Christianson, D. D. (1982). Swelling capacity of starch and its relationship to suspension viscosity. Effect of cooking time, temperature and concentration. *Journal of Texture Studies, 13*, 115–126.

Casson, N. (1959). A flow equation for pigment–oil suspensions of the printing ink type. In C. C. Mill (Ed.), *Rheology of Disperse Systems* (pp. 82–104). New York: Pergamon Press.

Chen, J., & Jane, J. (1994). Preparation of granular cold-water-soluble starches by alcoholic-alkaline treatment. *Carbohydrates, 71*(6), 618–622.

Christianson, D. D., Hodge, J. E., Osborne, D., & Detroy, R. W. (1981). Gelatinization of wheat starch as modified by xanthan gum, guar gum, and cellulose gum. *Cereal Chemistry, 58*(6), 513–517.

Dzuy, N. Q., & Boger, D. V. (1983). Yield stress measurement for concentrated suspensions. *Journal of Rheology, 27*, 321–349.

Eastman, J. E., & Moore, C. O. (1984). Cold-water-soluble granular starch for gelled food compositions. *U.S. Patent 4, 465, 702*.

Eidam, D., Kulicke, W. M., Kuhn, K., & Stute, R. (1995). Formation of maize starch gels selectively regulated by the addition of hydrocolloids. *Starch/Stärke, 47*(10), 378–384.

Genovese, D. B., & Rao, M. A. (2003a). Vane yield stress of starch suspensions. *Journal of Food Science, 68*, 2295–2301.

Genovese, D. B., & Rao, M. A. (2003b). Role of starch granule characteristics (volume fraction, rigidity, and fractal dimension) on rheology of starch dispersions with and without amylose. *Cereal Chemistry, 80*, 350–355.

Genovese, D. B., & Rao, M. A. (2005). Components of vane yield stress of structured food dispersions. *Journal of Food Science, 70*, E498–E504.

Gonera, A., & Cornillon, P. (2002). Gelatinization of starch/gum/sugar systems studied by using DSC, NMR, and CSLM. *Starch/Stärke, 54*(11), 508–516.

Krüger, A., Ferrero, C., & Zaritzky, N. E. (2003). Modelling corn starch swelling in batch systems: Effect of sucrose and hydrocolloids. *Journal of Food Engineering, 58*, 125–133.

Langan, R. E. (1986). Food industry. In O. B. Wurzburg (Ed.), *Modified Starches: Properties and Uses* (pp. 199–212). Boca Raton, Florida: CRC Press, Inc..

Launay, B., Cuvelier, G., & Martinez-Reyes, S. (1984). Xanthan gum in various solvent conditions: intrinsic viscosity and flow properties. In G. O. Phillips, D. J. Wedlock, & P. A. Williams (Eds.), *Gums and Stabilizers for the Food Industry—2* (pp. 79–98). Oxford, UK: Paragon Press.

Mandala, I. G., & Palogou, E. D. (2003). Effect of preparation conditions and starch/xanthan concentration on gelation process of potato starch systems. *International Journal of Food-Properties, 6*, 311–328.

Mandala, I. G., Palogou, E. D., & Kostaropoulos, A. E. (2002). Influence of preparation and storage conditions on texture of xanthan–starch mixtures. *Journal of Food Engineering, 53*, 27–38.

Meng, Y., & Rao, M. A. (2005). Rheological and structural properties of cold-water-swelling and heated cross-linked waxy maize starch dispersions prepared in apple juice and water. *Carbohydrate Polymers, 60*(3), 291–300.

Metz, B., Kossen, N. W. F., & Suijdam, J. C. (1979). The rheology of mould suspensions. In T. K. Ghose, A. Fiechter, & N. Blakebrough (Eds.). *Advances in Biochemical Engineering* (Vol. 2, pp. 103–156). New York: Springer-Verlag.

Michaels, A. S., & Bolger, J. C. (1962). The plastic flow behavior of flocculated kaolin suspensions. *Industrial and Engineering Chemistry Fundamentals, 1*, 153–162.

Miles, M. J., Morris, V. J., Orford, P. D., & Ring, S. G. (1985). The roles of amylose and amylopectin in the gelation and retrogradation of starch. *Carbohydrate Research, 135*, 271–281.

Nayouf, M., Loisel, C., & Doublier, J. L. (2003). Effect of thermomechanical treatment on the rheological properties of cross linked waxy corn starch. *Journal of Food Engineering, 59*, 209–219.

Nguyen, Q. D., Jensen, C. T. B., & Kristensen, P. G. (1998). Experimental and modeling studies of the flow properties of maize and waxy maize starch pastes. *Chemical Engineering Journal, 70*, 165–171.

Okechukwu, P. E., & Rao, M. A. (1995). Influence of granule size on viscosity of cornstarch suspension. *Journal of Texture Studies, 26*, 501–516.

Qiu, C. G., & Rao, M. A. (1988). Role of pulp content and particle size in yield stress of apple sauce. *Journal of Food Science, 53*, 1165–1170.

Rao, M. A. (1999). *Rheology of fluid and semisolid foods: Principles and applications*. Gaithersburg, MD: Aspen Publishers.

Rao, M. A., & Cooley, H. J. (1984). Determination of effective shear rates of complex geometries. *Journal of Texture Studies, 15*, 327–335.

Ring, S. G., & Stainsby, G. (1982). Filler reinforcement of gels. *Progress in Food and Nutrition Science, 6*, 323–329.

Tattiyakul, J., & Rao, M. A. (2000). Rheological behavior of cross-linked waxy maize starch dispersions during and after heating. *Carbohydrate Polymers, 43*, 215–222.

van den Tempel, M. (1961). Mechanical properties of plastic disperse systems at very small deformations. *Journal of Colloid Science, 16*, 284–296.

Wang, F., Sun, Z., & Wang, Y. J. (2001). Study of xanthan gum/waxy corn starch interaction in solution by viscometry. *Food Hydrocolloids, 15*(4–6), 575–581.

Whistler, R. L., & BeMiller, J. N. (1997). *Carbohydrate chemistry for food scientists*. St. Paul, Minnesota: Eagan press, 91–151 and 179–185.